Available online at www.sciencedirect.com
ScienceDirect
International Journal of Mass Spectrometry 258 (2006) 134–141
International Journal of Mass Spectrometry
www.elsevier.com/locate/ijms

The preparation of <100 particles per trial having the same mole fraction of 12 inorganic compounds at diameters of 6.8, 3.8, or 2.6 μm followed by their deposition onto human lung cells (A549) with measurement of the relative downstream differential expression of ICAM-1

Ndukauba M. Eleghasim [a], Allen E. Haddrell [a], Stephen van Eeden [b], George R. Agnes [a,*]

[a] *Department of Chemistry, Simon Fraser University, 8888 University Drive, Burnaby, British Columbia, Canada V5A 1S6*
[b] *James C Hogg iCAPTURE Centre for Cardiovascular & Pulmonary Research, University of British Columbia, Vancouver, British Columbia, Canada V6Z 1Y6*

Received 17 May 2006; received in revised form 16 July 2006; accepted 18 July 2006
Available online 21 August 2006

Abstract

The characterization of particulate matter suspended in the troposphere (PM_{10}) based on size is an important basis for assessing the extent of their adverse effects on human health. The relevance of such assessments is anticipated to be significantly improved through the continued development of tools that can identify the chemical components within individual ambient particles, and the injury that they cause. We use recently reported methodology to create mimics of ambient particle types of known size and chemical composition that are levitated within an ac trap. The ac trap uses electric fields to levitate the particles that have a given mass and net elementary charge, and as such the ac trap is a mass-to-charge filter. The ac trap was used to levitate populations of particles where the size of particles in any given population could be altered. The levitated particles are delivered direct from the ac trap to human lung cells (A549), *in vitro*, with downstream measurement of differential expression of intercellular adhesion molecule (ICAM)-1 and counting of the number of particles actually delivered to the culture using an optical microscope. In this study, the chemical composition of the ambient particle mimics was restricted to inorganic compounds whose relative abundance was purposely designed to mimic the average abundance in Environmental Health Center-93 (EHC-93) particles. The sizes of the multilelement particle types prepared were 6.8 ± 0.5, 3.8 ± 0.3, 2.6 ± 0.2 (mean ± S.D.). Particles of either elemental carbon, or elemental carbon containing glycerol were used as control particle types. In any given experiment, a known number of particles, but always <100, of a given size, were deposited onto a small region of an A549 cell culture. Following an 18-h incubation period and anti-body labeling of ICAM-1, the fluorescence emission from a 1.07 mm^2 area of the cell culture centered at the site of particle deposition was acquired. The relative differential expression of ICAM-1 was greatest for multielement particle types having diameters of 2.6 ± 0.2 μm for which as few as ∼15 particles deposited onto the culture resulted in maximal ICAM-1 expression, whereas with multielement particle types having diameters of 6.8 ± 0.5 μm, it was necessary to deposit >50 particles in order to effect comparable ICAM-1 expression. This data set indicates that for multi-element particle types comprised of the same mole fraction of inorganic compounds and of sizes within the course fraction of PM_{10}, the 2.6 μm particle type was the most potent with respect to effecting differential expression of ICAM-1.
© 2006 Elsevier B.V. All rights reserved.

Keywords: Particulate matter; Inorganic compounds; ac trap levitation; ICAM-1; Inflammation potential

1. Introduction

Epidemiological studies positively correlate ambient particle concentrations to increased frequency of hospital admissions [1–5]. It is speculated that inflammation, ranging in severity between localized within lung tissue to systemic is the biological connection linking ambient particle exposure to the pathogenesis of respiratory and cardiovascular diseases [6–12]. Regulations specify exposure limits to particulate matter with aerodynamic diameters less than 10 μm (PM_{10}) and 2.5 μm ($PM_{2.5}$), respectively [13–15]. Small reductions in ambient particulate matter concentrations achieved through reasonable and attainable

* Corresponding author. Tel.: +1 604 291 4387; fax: +1 604 291 3765.
E-mail address: gagnes@sfu.ca (G.R. Agnes).

1387-3806/$ – see front matter © 2006 Elsevier B.V. All rights reserved.
doi:10.1016/j.ijms.2006.07.010

strategies are predicted to yield substantial returns with respect to reduced health care cost.

While it is understood from aerodynamic modeling studies that fine fraction ambient particles ($PM_{2.5}$) penetrate deep into the alveolar region of the respiratory tract, and coarse fraction ambient particles ($PM_{2.5}$–PM_{10}) tend to be most important for the upper region of the airway [16], it is not yet well characterized what actual particle chemical composition causes the most injury [17–20]. Further complicating this issue is that the chemical compositions of various size fractions vary based on source, tropospheric processing, and season [21]. This has been an impetus for developing tools to characterize the chemical composition of individual ambient particles. The challenges in contributing new knowledge in this area are formidable, as evidenced by the number of studies that report different conclusions regarding a single known component of ambient particle types, such as endotoxin from gram-negative bacteria [22–24].

Prior studies performed by other investigators have used particle models, including polystyrene beads, titanium dioxide, and carbon black to mimic various particulate matter size fractions [25,26]. However, the chemical composition of such models of ambient particles might not be relevant mimics of actual ambient particles. In contrast, other toxicology studies have used actual ambient particles collected from the troposphere [27]. A chemically well characterized sample of ambient particles, now referred to as Environmental Health Center-93 (EHC-93), is an example of a heterogeneous population of particles being used in toxicology studies in which the whole particle, and its soluble and insoluble fractions have been characterized [28–30]. EHC-93 is comprised of metals, inorganic compounds, and organic compounds [31,32] with 99% of its size fraction being <3 μm [33]. Studies involving EHC-93 report the mass of particles introduced to a cell culture, but not the actual size and number of particles interacting with any given cell. Also, the chemical composition of the individual particles in EHC-93 are not characterized, so it is difficult to extrapolate from those studies what individual particle compositions are most significant with respect to their role in causing tissue inflammation. Such information could be important with respect to effecting rational strategies to reduce emissions of the specific compounds identified as being most significant in particulate air pollution. With respect to addressing these issues of particle chemistry, we have reported a laboratory apparatus that enables the design of multi-component particles that mimic those found, or speculated to exist in the troposphere, and deposit those particles directly onto human lung cells, *in vitro*.

Ambient particles of different sizes are likely to have different chemical composition, but within the same size fraction, it is probable that there are particle types having similar composition. To learn of the extent of the relative injury reported by a cell culture in response to incubation with different sizes of a given particle type, we chose to prepare particles having a chemical composition similar to the bulk, or average, inorganic composition of EHC-93. The relative injury reported by cells in these experiments was quantified based on the differential expression of the pro-inflammatory membrane glycoprotein intercellular adhesion molecule (ICAM)-1.

The clearance of inhaled particles from the respiratory system has been shown to be mediated by the respiratory epithelium whose action constitutes one of the body's inflammatory responses [34]. Recent studies have shown this inflammatory mechanism involves the recruitment and migration of leukocytes, mainly neutrophils, through the endothelium to the site of inflammation [35]. The leukocyte recruitment and migration requires the surface expression of an adhesive glycoprotein (ICAM)-1, which interacts with CD18/β_2-integrin-containing receptors on neutrophils [36,37].

2. Materials and methods

2.1. Starting solutions

Each of the particle types created and used consisted of the dissolved solids, and elemental carbon nanoparticles, that had been introduced to each of the starting solutions used.

The procedure for the preparation of a multielement starting solution first required the preparation of single component stock solutions using reagent grade compounds. Aliquots from the single component stock solutions were combined to yield what is referred to as the multielement starting solution (Table 1). The amount of elemental carbon in EHC-93 is not reported in the literature [31,32], however, previous studies have indicated that elemental carbon generally constitutes approximately 10% by mass of particulate matter [38,39]. That result was used to establish the mass of elemental carbon nanoparticles in Indian ink added to the multi-element starting solution. To this solution, Indian ink (Speedball, Product no. 3328, Statesville, NC, USA) was added as the source of elemental carbon nanoparticles. Three millilitres of India Ink, corresponding to ∼0.45 g elemental carbon nanoparticles, was added to 6.50 mL of multielement solution. The elemental carbon nanoparticles facilitated visualization and counting of the multielement particle type deposited onto each cell culture following immunocytochemistry assay. Serial dilution of the multielement starting solution

Table 1
The concentrations of inorganic compounds in the multielement starting solution from which multielement particle types were prepared

Inorganic Compound	Concentration (mol/L)
$CaSO_4$	6.5×10^{-5}
$BaSO_4$	3.7×10^{-7}
$SrSO_4$	3.6×10^{-4}
$Cr_2(SO_4)_3 \cdot H_2O$	1.5×10^{-4}
$3CdSO_4 \cdot 8H_2O$	3.6×10^{-5}
$CuSO_4 \cdot 5H_2O$	2.4×10^{-3}
$VOSO_4 \cdot 2H_2O$	3.3×10^{-4}
Na_2SO_4	1.7×10^{-1}
$MgSO_4 \cdot 7H_2O$	5.4×10^{-2}
$Al_2(SO4)_3 \cdot 18H_2O$	6.7×10^{-2}
$FeSO_4 \cdot 7H_2O$	4.9×10^{-2}
$CoSO_4 \cdot 7H_2O$	1.6×10^{-5}
$Zn(NO_3)_2 \cdot 6H_2O$	2.9×10^{-2}
$Ni(NO_3)_2 \cdot 6H_2O$	2.2×10^{-4}
$Mn(NO_3)_2$	1.6×10^{-3}
$PbCl_2$	2.1×10^{-5}

to which elemental carbon nanoparticles had been added was performed as indicated in preparing other multielement solutions having lower ionic strength.

A different set of three starting solutions consisted of India Ink in distilled deionized water were prepared with 1 μL India Ink in 10 μL water, 1 μL India Ink in 400 μL water, and 1 μL India Ink in 2.42 mL water. The particles prepared using these starting solutions are referred to as elemental carbon particle types, but note that these particle types differ in chemical composition relative to soots released in the exhaust of high temperature combustion sources. Another starting solution consisted of glycerol:water at 5:95 (v/v) with 3.0 mL of India Ink, corresponding to ~0.45 g elemental carbon nanoparticles, in 6.50 mL water.

2.2. Cell culture

A549 human lung epithelial cell line (American type culture collection, Manassas, VA, USA), derived originally from lung tissue of a male tumor patient, has the characteristics of type-II alveolar cells of the human pulmonary epithelium [40]. This cell line has been used extensively in studies of particulate matter-induced responses via ICAM-1 expression [41]. Cells were seeded at a density of 2×10^5 cells per well in six-well culture plates containing minimum essential medium (MEM), supplemented with 10% heat inactivated fetal bovine serum (FBS), 1% L-glutamine, and 1% MEM vitamin solution. Cells were grown to >95% confluency at 37 °C, in an atmosphere containing 5% CO_2 and 100% relative humidity.

Cell cultures that served as positive controls contained 2 mL of growth medium to which 10 μL of 1 mg/mL of tumor necrosis factor alpha (TNF)-α (Sigma–Aldrich, T6674-10UG, Oakvillle, Ont., Canada) in water was added [42,43]. Cell cultures that served as negative controls were bathed in growth medium only.

2.3. Droplet dispensing

Each particulate mimic was derived from a monodisperse droplet dispensed from a droplet dispenser loaded with a starting solution. The dispensed droplets were trapped in an ac trap and levitated while the volatile solvent evaporated causing the dissolved solids to precipitate [44,45].

To prepare particles of varying sizes, 0.5 mL aliquots of the multielement starting solution were taken and diluted with 7.5, 12.5, and 25.0 mL of distilled deionized water, to generate secondary multielement solutions that had ionic strengths of 0.103, 0.092 and 0.045 M respectively.

The levitation chamber that housed the ac trap was placed in a biological safety cabinet (Nuaire Inc., Model Nu-425-600, Plymouth, MN, USA). A schematic diagram of the ac trap with the major components indicated is shown in Fig. 1A. The internal reservoir of the 60 μm-diameter droplet dispenser (MicroFab Technologies Inc., MJ-AB-01-60, Plano, TX, USA) was filled with an aliquot of a starting solution using a 10 μL pipette. To dispense a droplet, the waveform generator for the droplet dispenser was programmed to dispense a set number of droplets at a set frequency. The electrical pulses from this waveform generator were used to actuate a cylindrical piezoceramic element bonded to the outside of the droplet dispenser reservoir and cause a small volume of liquid to be ejected from the dispenser nozzle as a jet. Care was exercised to ensure monodisperse droplet dispensing.

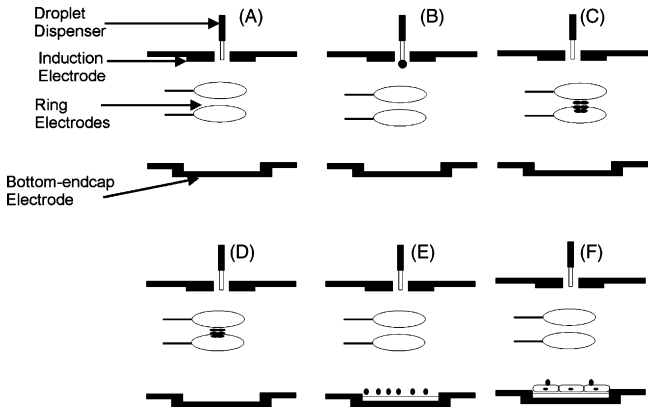

Fig. 1. A representation of the levitation apparatus used in the creation and deposition of particles onto two different surfaces. (A) Schematic diagram of the ac trap with the major components indicated by the labels. A 10 μL aliquot of a multielement starting solution is used to load the internal reservoir of the droplet dispenser. (B) Dispensing of a droplet. (C) Levitation of a population of droplets while the volatile solvents present in the starting solution evaporate. (D) Levitation of the resultant particles formed by the precipitation of the dissolved solids present in the starting solution. (E) Particle deposition onto glass slide for size characterization using optical microscopy. (F) Particle deposited onto a A549 cell culture. Diagram is not to scale.

A dc potential applied to an induction electrode positioned 2 mm below the droplet dispenser nozzle caused charge imbalance within the liquid jet. The momentum of the jet caused it to separate and collapse to form a droplet, and the charge imbalance in the jet resulted in each droplet having a net charge (Fig. 1B). Droplets were dispensed downwards into the ac trap that was used to levitate the droplets.

2.4. Particle levitation in an ac trap and measurement of particle diameter

The ac trap used is an imperfect electrodynamic balance (EDB). The ac trap has many similarities to a Paul trap, also known as a three dimensional quadrupole ion trap mass spectrometer [46], and as such, the ac trap is a mass-to-charge filter [47,48]. The frequency of the ac trap was adjusted, in conjunction with the ionic strength of the multielement starting solution, or also the concentration of elemental carbon nanoparticles in other starting solutions described in Section 2.1, to effect levitation of particle populations having different sizes.

The droplets dispensed from the droplet generator fly into the ac trap through a 5-mm diameter hole in the induction electrode (Fig. 1C). Within the ac trap, a sinusoidal waveform, 130 Hz, 4.5 $kV_{0\text{-}P}$, applied to the ring electrodes established an electric field that enabled the droplets to be levitated in air. The volatile components evaporate within seconds from the levitated droplet causing the non-volatile components in each droplet

to precipitate and coagulate as a spherical particle (Fig. 1D). The actual distribution of the compounds in these particles has not been characterized. Though the motion of the levitated droplets/particles is collisionally dampened because of the high pressure at which these experiments were performed (1 atm), it is necessary to maintain the magnitude of the dimensionless parameter q for a trapped droplet/particle approximately constant. The q-value for a charged object trapped by an electric field relates the droplet/particle mass-to-charge value to the square of the ac waveform frequency in addition to other factors describing the dimensions of the electrodes. In practice, manually increasing the frequency of the ac waveform applied to the ring electrodes of the ac trap during the period over which volatile solvent evaporates from the levitated droplets allows crude tracking of the loss of mass from the levitated droplet. Imperfect electrode dimensions that introduce higher order fields, and collisional pressure dampening of the levitated particle, are key factors that enable the retention of a population of levitated droplets with each droplet having its own different mass-to-charge value in the ac trap during the period of time over which volatile solvent evaporates. The end frequency necessary to maintain a population of particles levitated was dependent on the resulting size of the particle that in turn depended on the ionic strength of the multielement solution from which the original droplet was dispensed. For multielement particle types that were 6.8, 3.8, 2.6, 1.8, and 1.4 μm diameter, the final ac frequency was 510, 810, 910, 1010, and 1230 Hz, respectively.

Following the formation of these particles, an attractive 500 V dc potential applied to the bottom electrode of the ac trap facilitated the removal of the particles from the trap. In one phase of the experiment, particles removed from the ac trap were collected on 75 mm × 25 mm glass slides (Fig. 1E) and the diameters of the roughly spherical-shaped particles measured using a calibrated optical microscope.

2.5. Particle deposition onto A549 human lung epithelial cell culture

The procedure and conditions in the ac trap described above for the dispensing of droplets and subsequent levitation of particles, whose diameters were characterized, was used without alteration for particles that were deposited onto A549 cell cultures. Upon levitation of a population of 5–100 particles, a culture of A549 cells was prepared as follows. First, the growth medium was drained and the 18 mm × 18 mm glass cover slip supporting the monolayer of A549 cells was placed on a 75 × 25 mm glass slide (Surgipath Inc., #00375, Winnipeg, Man., Canada). The glass slide was then placed on a mount that sat on the bottom electrode. A 500 V dc potential applied to the bottom electrode established an attractive force that enabled the particles to be removed from the EDB and impact onto the cell culture positioned directly below the ring electrodes of the ac trap (Fig. 1F). After the deposition of the particles, the 18 mm × 18 mm glass cover slip was immediately transferred into a 35 mm (diameter) × 10 mm (depth) tissue culture petri dish (Sarstedt Inc., Model #28658-0468, Newton, NC, USA) and incubated at 5% CO_2, 37 °C, and 100% relative humidity for 18 h.

2.6. Immunocytochemistry assay

After an 18-h incubation period, an antibody assay was performed in a biological safety cabinet as follows. The monolayer of A549 cells was twice washed with 1 mL phosphate-buffered saline (PBS) solution. The cell culture was then fixed with 1 mL of 1% acetone solution and allowed to stand for 10 min and afterwards discarded. After acetone fixation, the cell culture was treated with 95 μL serum-free protein block, reported by the manufacturer as having 0.25% casein in PBS, stabilizing proteins and 0.015 mol/L sodium azide (DakoCytomation Inc., X0909, Carpinteria, CA, USA) for 30 min, followed by treatment with 95 μL of 50 μg/0.5 mL solution of mouse-antihuman monoclonal CD54 primary antibody (Caltag Laboratories, LMHCD54F, Burlingham, CA, USA) for 1 h.

After the 1 h treatment with the primary antibody, the cell culture was washed with 1 mL of tris-buffered saline solution (TBS) and then incubated with 95 μL of 2 mg/mL solution of goat-antimouse IgG secondary antibody solution conjugated to Alexa Fluor 546 (Invitrogen Detection Technologies, 34779A, Eugene, OR, USA) for 30 min. At 30 min treatment with this secondary antibody, the cell culture was washed four times with TBS solution prior to performing fluorescence microscopy and image analysis.

The positive control were cultures that had been incubated with tumor necrosis factor (TNF)-α. To 2 mL of growth medium bathing an A549 culture grown to confluence on an 18 mm × 18 mm glass cover slip, 10 μL of 10 μg/mL TNF-α solution was added and then incubated for 18 h followed by immunocytochemistry as described above. Negative controls were A549 cultures grown to confluence on 18 mm × 18 mm glass cover slips bathed with 2 mL of growth medium and then incubated for 18 h followed by immunocytochemistry as described above.

2.7. Fluorescence microscopy and analysis of acquired images

All images of fluorescence emission from the fluorescently tagged antibodies bound to ICAM-1 expressed on A549 cells were collected with an inverted fluorescence microscope equipped with an Epi-fluorescence filter block (filter block model MG-1, Epi-FI, microscope model AE31, Motic Instruments Inc., Richmond, BC, Canada). The deposition site scan is defined as a 1 mm^2 circular area centered over the site of particle deposition from which fluorescence emission was collected. Differential ICAM-1 expression was calculated based on the fluorescence emission signal intensity at each pixel in each scan of a cell culture using Image J software (Research Services branch, National Institute of Health, Bethesda, MD, USA) and the numerical values of the pixel signals were summed using Microsoft Excel. The summed ICAM-1 expression is reported as a percent of total signal intensity relative to A549 cell cultures treated with TNF-α as the positive control [45].

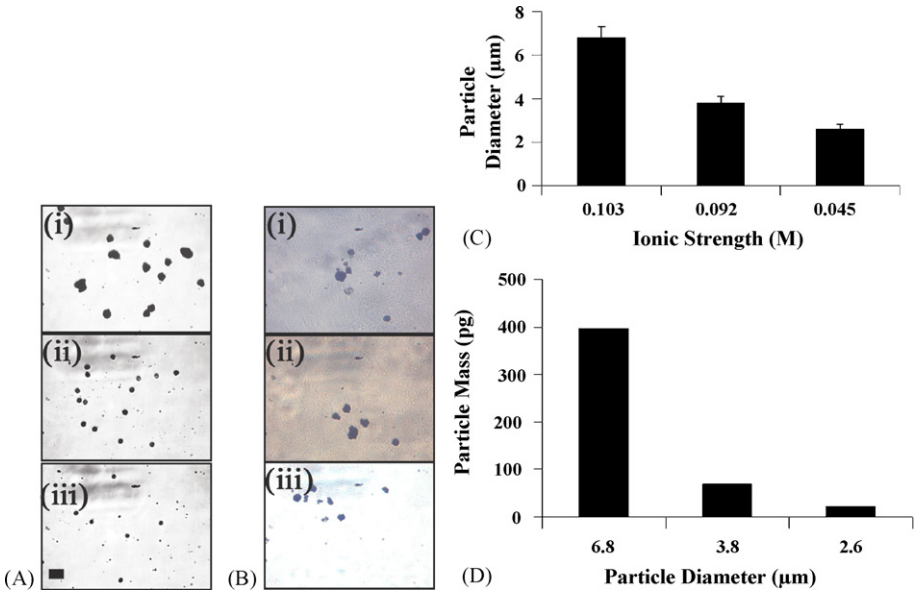

Fig. 2. (A). Representative photomicrographs of multielement particle types that were deposited onto glass slides for size characterization using optical microscopy. Their average diameters were (i) 6.8 μm, (ii) 3.8 μm, and (iii) 2.6 μm. (B) Representative photomicrographs of multielement particle types that had been deposited onto A549 cell cultures and visualized following an 18-h incubation period. The scale bar in panel A (iii) represents 15 μm and it is valid for all images. (C) Bar graph representation of the diameters of the multielement particles formed in the ac trap as a function of the ionic strength of the multielement starting solution. (D) The mass of inorganic compounds contained in each size of the multilelement particle type created.

3. Results

3.1. Characterization of particle diameter

Ac traps have been used in many studies involving the levitation of droplets containing inorganic compounds [49]. In this work, multi-compound containing droplets were captured in the ac trap and levitated for 1 min to allow the dissolved solids to precipitate. The multielement particles thus formed were then deposited onto a glass cover slip. Photomicrographs of each size of these particles as viewed using an optical microscope are presented in Fig. 2A, panels i–iii. The average diameter of each particle type generated from the multielement starting solution having ionic strengths of 0.103, 0.092 and 0.045 M were 6.8 ± 0.5, 3.8 ± 0.3, 2.6 ± 0.2 μm, respectively (mean ± S.D.). The relative sizes of these particles are depicted in bar-graph format in Fig. 2C, and their per particle mass in Fig. 2D. Not shown are the images of the elemental carbon and elemental carbon containing glycerol particle types that were similarly characterized.

Representative photomicrographs of these same particle sizes following their deposition onto A549 cell cultures and an incubation period of 18-h are shown in Fig. 2B, panels i–iii. While the preparation and deposition of particles having diameters of <2.5 μm was achieved (data not shown), those particle sizes were broken down following an 18 h incubation to the extent that no visible remnants of the particles were distinguishable. A technical issue regarding our use of particles <2.5 μm diameter is the capability to count the number of particles actually deposited. Work is underway to calibrate an in-house assembled optical particle counter.

3.2. Inflammation potential of a multielement inorganic particle type using particle diameters of 6.8, 3.8, and 2.6 μm

The apparatus used to create and deliver particles to cultures in these dose-response experiments allows us to know the number, size, and composition of the particles deposited. With respect to the cellular response, the injury monitored was limited to the quantitative measurement of the differential expression of a single pro-inflammatory mediator, ICAM-1. The expression of ICAM-1 in all test cultures was normalized using the positive control. The cultures used as negative controls were also normalized to the positive controls and the relative expression of ICAM-1 measured in those was ~0.4.

Each data point in Fig. 3 is the fluorescence signal intensity measured at the site of particle deposition, and that value is taken as the differential expression of ICAM-1 relative to the positive control from each experiment. The data showing the fluorescence from cultures dosed with elemental carbon particles that were themselves 6.7, 3.8, and 2.7 μm in diameter are plotted as open symbols in Fig. 3. The elemental carbon particles did not cause measurable differential expression of ICAM-1 in A549 cells relative to the negative control. Also, elemental carbon containing glycerol particles that were 6.8 μm in diameter were also dosed onto A549 cultures, and the immunocytochemistry data indicated that ICAM-1 expression was not significantly different than that in the negative controls (data not shown). The mass of elemental carbon in the elemental carbon containing glycerol droplets was the same as in the multielement particle types that were also dosed onto A549 cultures (Fig. 3, closed symbols). Clearly, the addition of the inorganic compounds, in the relative quantities indicated in Table 1, to elemental carbon to create a

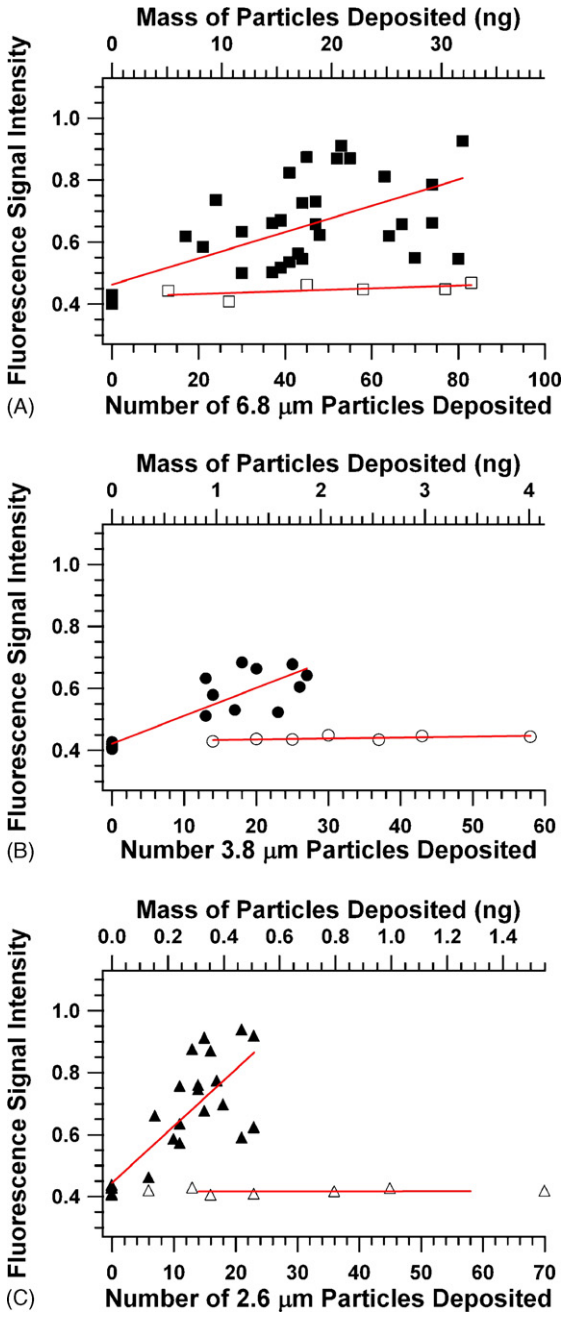

Fig. 3. Relative fluorescence signal intensity of fluorophore-tagged secondary antibodies of goat-antimouse bound to ICAM-1 expressed on A549 cell culture after an 18 h incubation with different numbers of different particle types having nominal diameters of (A) 6.8 μm, (B) 3.8 μm, and (C) 2.6 μm. Bottom *x*-axis represents the number of particles of the indicated size delivered to the cell culture and the top *x*-axis represents the mass of particles delivered. Filled symbols represent multielement particle types having the same mole fraction of the same compounds, and open symbols represent elemental carbon particles. The fluorescence signal intensity was collected from a 1.07 mm^2 area centered over the site of particle deposition. The R^2 coefficient from the linear least squares fit to the fluorescence signal intensity versus the number of multielement particles deposited (filled symbols) was (A) 0.6, (B) 0.6 and (C) 0.8.

multielement particle type resulted in differential expression of ICAM-1.

The relative fluorescence signal intensity data in the images of the cell cultures following immunocytochemistry, indicative

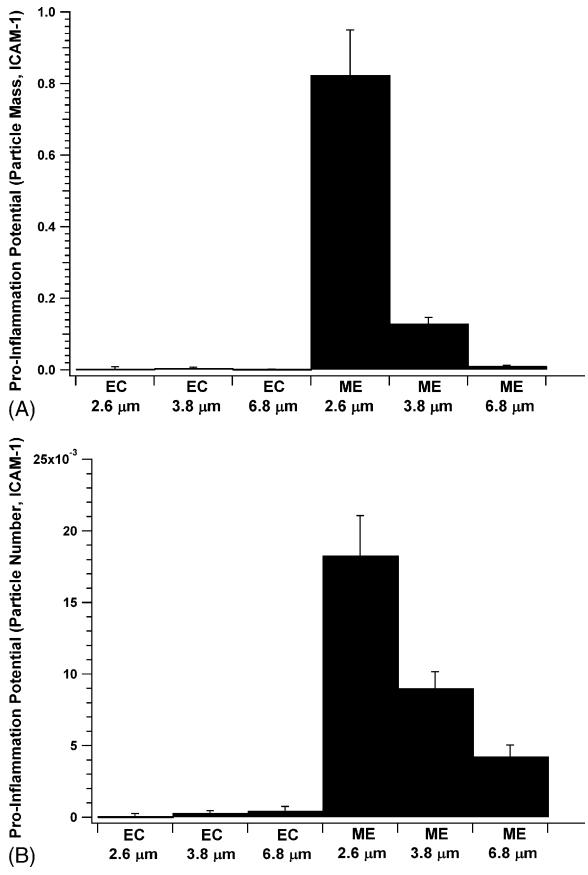

Fig. 4. Pro-inflammation potential (PIP) displayed as a function of the differential expression of ICAM-1 in response to incubation with elemental carbon (EC) or multielement (ME) particle types having the indicated diameter in micrometers. The data set is presented in two formats; in (A) the PIP was calculated as a function of the mass of particles delivered to the cultures, and (B) the PIP was calculated as a function of the number of particles delivered to the cultures.

of the relative ICAM-1 expression in Fig. 3, were fitted to least squares linear regressions as a function of the mass and as the number of multielement and carbon particle types delivered. The value of the slopes to these fits are presented in bar-graph format in Fig. 4 and the error bars indicate the error in the fitted slope. The magnitude of the numerical values for the slope of the least squares linear fits are interpreted as the pro-inflammation potential (ICAM-1) for a given size of a given particle type.

4. Discussion

This study utilized an apparatus and associated methodology with which questions at the interface between atmospheric particle chemistry and lung cell biology can be addressed. For example, the data generated with this infrastructure allows the data to be presented in a format that enables inter-comparison between composition, number, and size of particles actually delivered to cell cultures for the purpose of identifying which components on different ambient particle types are most significant with respect to causing adverse effects on human health. Clearly the type (e.g.: chemical composition), size, and number of particles delivered to a culture are significant factors in characterizing the relative injury, in vivo, caused by ambient

particle types (Fig. 4). Our results indicate that particles having varying sizes but the same bulk inorganic chemical composition effected a different level of injury to A549 cells based on the measured differential ICAM-1 expression. As few as ∼15 multi-element particles of diameter 2.6 μm caused significant ICAM-1 expression whereas with 6.8 μm diameter particles having the same mole fraction of multiple compounds >50 such particles were required to initiate a significant response. Moreover, different sizes of a control particle type, elemental carbon, were measured to have induced no differential expression of ICAM-1 relative to the negative controls.

Prior studies have indicated that the fine fraction particles (i.e. $PM_{2.5}$) were more toxic than coarse fraction ambient particles (i.e. PM_{10}–$PM_{2.5}$) [50,51]. This could simply be due to more favorable particle-cell interaction (i.e. rate of endocytosis) for the smaller particle size studied, and not a function of particle chemical composition. The extent to which the varied compounds contribute to toxicities of coarse and fine fractions of ambient particles following inhalation exposure is not well understood, as significant differences exist between coarse and fine fractions regarding their sources, chemical compositions, atmospheric life times and temporal variability. The question remains, what particle physicochemical properties contribute most significantly to the observed inflammation following inhalation exposure to particulate matter of varying size fractions? Particulate matter has been shown to generally contain numerous chemical components that include elemental carbon, metals, inorganic compounds and organic compounds [39]. Furthermore, coarse fraction particulate matter contains endotoxin, and several studies have suggested that these particle types are significant contributors to particulate air pollution. While conclusions should not be drawn at this stage regarding the role of chemical components on fine versus coarse fraction ambient particles and their potency with respect to causing tissue injury, hypotheses can however be formulated to address this issue regarding particulate air pollution using the apparatus and associated methodology described herein. Note that the results presented involved particles within the coarse fraction of ambient particles. An extension of this data set using the same multi-element particle types into the fine fraction of ambient particles could be informative because for such particles sizes the particle–cell interactions could be less dissimilar, and particle surface area or surface area of reactive sites on a particle could be important [17].

A hypothesis regarding nanoparticle toxicity postulates that their surface area could be a very important factor in determining the extent of the injury that they cause [52]. In order for our data to have been in agreement with that nanoparticle surface-area hypothesis, a similar relative injury caused on a per particle surface area basis would have had the ICAM-1 expression caused by a single 6.8 μm diameter particle being approximately similar to that caused by a calculated seven particles of 2.6 μm diameter. This was not what was observed, and therefore these results on coarse fraction ambient particle types ($PM_{2.5}$–PM_{10}) should not be extrapolated to the nanometer size regime. When quantitative dose-response methodology has been developed to the extent that particles of size within the $PM_{2.5}$ classification can be used and the relative cellular injury inter-compared, a test of the nanoparticle surface area hypothesis for fine fraction ambient particles ($PM_{2.5}$) could be performed.

Work is underway to characterize the pro-inflammation potential of (i) particles that lack several of the inorganic compounds reported herein, (ii) particles that contain organic compounds in addition to the inorganic compounds used herein, spanning from volatile organic hydrocarbons to endotoxin, and (iii) particles whose diameters are <2.5 μm. Such future work can be expected to assist in evaluation of the relative necessity to have knowledge of the chemical composition of ambient particles types, in addition to their number and size, in order to fully predict and therefore mitigate inhalation exposure risk.

5. Conclusion

A particle levitation apparatus and associated methodology was used to design a multielement particle type that was created at different sizes within the coarse fraction of PM_{10} but all with the same chemical composition that represented the bulk inorganic composition of EHC-93. Based on the number of multielement particles deposited, particles of 2.6 μm in diameter were respectively, two and four times more potent in causing cellular up-regulation of ICAM-1 than particles of 3.8 and 6.8 μm in diameter in terms of number of particles deposited. The same data, evaluated based on the mass of particulate material delivered to a culture, indicated that the 2.6 μm diameter particle type was, respectively, 6 and 80 times more potent in terms of effecting cellular up-regulation of ICAM-1 versus the 3.8 and 6.8 μm diameter particles. These results illustrate there is need to have detailed knowledge of individual particle composition, number and size comprising the cumulative particulate matter delivered to tissue in order to more accurately evaluate potential health outcomes associated with inhalation exposure to ambient particles.

Acknowledgements

The British Columbia Lung Association, The Canadian Foundation for Climate and Atmospheric Sciences (CFCAS), and the Natural Science and Engineering Council of Canada (NSERC) funded this research. Dr. Stephan van Eeden is an American Lung Association Career Investigator and the William Thurlbeck Distinguished Researcher.

References

[1] J.M. Samet, F. Dominici, F.C. Curriero, I. Coursac, S.L. Zeger, New Engl. J. Med. 343 (2000) 1742.
[2] R.T. Burnett, R. Dales, D. Krewski, R. Vincent, T. Dann, J.R. Brook, Am. J. Epidemiol. 142 (1995) 15.
[3] D.V. Bates, M. Bakeranderson, R. Sizto, Environ. Res. 51 (1990) 51.
[4] J. Schwartz, D. Slater, T.V. Larson, W.E. Pierson, J.Q. Koenig, Am. Rev. Respir. Dis. 147 (1993) 826.
[5] D.V. Bates, R. Sizto, Environ. Res. 43 (1987) 317.
[6] R.B. Brook, B. Franklin, W. Cascio, Y. Hong, G. Howard, M. Lipsett, R. Luepker, M. Mittleman, J. Samet, S.C. Smith, I. Tager, Circulation 109 (2004) 2655.
[7] P. Libby, Nature 420 (2002) 868.

[8] C.A. Pope, R.T. Burnett, G.D. Thurston, M.J. Thun, E.E. Calle, D. Krewski, J.J. Godleski, Circulation 109 (2004) 71.
[9] B. Brunekreef, J. Occup. Environ. Med. 54 (1997) 781.
[10] R.B. Hetland, F.R. Cassee, M. Refsnes, P.E. Schwarze, M. Lag, A.J.F. Boere, E. Dybing, Toxicol. In Vitro 18 (2004) 203.
[11] P.S. Gilmour, I. Rahman, S. Hayashi, J.C. Hogg, K. Donaldson, W. MacNee, Am. J. Physiol. Lung Cell Mol. Physiol. 281 (2001) L598.
[12] A. Nel, Science 308 (2005) 804.
[13] D. Zmirou, A. Deloraine, F. Balducci, C. Boudet, J. Dechenaux, J. Occup. Environ. Med. 41 (1999) 847.
[14] M.A. Deluchi, J.J. Murphy, D.R. McCubbin, J. Environ. Manage. 64 (2002) 139.
[15] K.K. Zaim, Environ. Manage. 23 (1999) 271.
[16] S. Anjivel, B. Asgharian, Fund. Appl. Toxicol. 28 (1995) 41.
[17] F.R. Cassee, H. Muijser, E. Duistermaat, J.J. Freijer, K.B. Geerse, J.C.M. Marijnissen, J.H.E. Arts, Arch. Toxicol. 76 (2002) 277.
[18] P.S. Gilmour, D.M. Brown, T.G. Lindsay, P.H. Beswick, W. MacNee, K. Donaldson, J. Occup. Environ. Med. 53 (1996) 717.
[19] J.A. Dye, J.R. Lehmann, J.K. McGee, D.W. Winset, A.D. Ledbetter, J.I. Everitt, A.J. Ghio, D.L. Costa, Environ. Health Perspect. 109 (2001) 395.
[20] R.P.F. Schins, J.H. Lightbody, P.J.A. Borm, T. Shi, K. Donaldson, V. Stone, Toxicol. Appl. Phamacol. 195 (2004) 1.
[21] K.F. Ho, S.C. Lee, C.K. Chan, J.C. Yu, J.C. Chow, X.H. Yao, Atmos. Environ. 37 (2003) 31.
[22] R. Burrell, R. Rylander, Environ. Res. 27 (1982) 325.
[23] I. Helander, H. Saxen, M. Salkinojasalonen, R. Rylander, Infect. Immunol. 35 (1982) 528.
[24] M.W. Baseler, B. Fogelmark, R. Burrell, Infect. Immunol. 40 (1983) 133.
[25] L.C. Renwick, D.M. Brown, A. Clouter, K. Donaldson, J. Occup. Environ. Med. 61 (2004) 442.
[26] D.M. Brown, M.R. Wilson, W. MacNee, V. Stone, K. Donaldson, Toxicol. Appl. Pharmacol. 175 (2001) 191.
[27] A.J. Ghio, Y.-C.T. Huang, Inhal. Toxicol. 16 (2004) 53.
[28] R. Vincent, P. Goegan, G. Johnson, J.R. Brook, P. Kumarathasan, L. Bouthillier, R.T. Burnett, Fundam. Appl. Toxicol. 39 (1997) 18.
[29] F.O. Omara, M. Fournier, R. Vincent, B.R. Blakley, J. Toxicol. Environ. Health Part A 59 (2000) 67.
[30] H. Ishii, S. Hayashi, J.C. Hogg, T. Fujii, Y. Goto, N. Sakamoto, H. Mukae, R. Vincent, S.F. van Eeden, Resp. Res. 6 (2005) 87.
[31] R. Vincent, S.G. Bjarnason, I.Y. Adamson, C. Hedgecock, P. Kumarathasan, J. Guenette, M. Potvin, P. Goegan, L. Bouthillier, Am. J. Path. 151 (1997) 1563.
[32] R. Biran, Y.Z. Tang, J. Brook, R. Vincent, G. Keeler, Int. J. Environ. Anal. Chem. 63 (1996) 315.
[33] T. Fujii, S. Hayashi, J.C. Hogg, R. Vincent, S.F. van Eeden, Am. J. Respir. Cell Mol. Biol. 25 (2001) 265.
[34] S.M. Travis, P.K. Singh, M.J. Welsh, Curr. Opin. Immunol. 13 (2001) 89.
[35] A.L. Humlicek, L.Y. Pang, D.C. Look, Am. J. Physiol. Lung Cell. Mol. Physiol. 287 (2004) L598.
[36] D.C. Look, S.R. Rapp, B.T. Keller, M.J. Holtzman, Am. J. Physiol. Lung Cell. Mol. Physiol. 263 (1992) L79.
[37] M.F. Tosi, J.M. Stark, C.W. Smith, A. Hamadani, D.C. Gruenert, M.D. Infeld, Am. J. Respir. Cell Mol. Biol. 7 (1992) 214.
[38] J.J. Schauer, J. Expos. Anal. Enviorn. Epidemiol. 13 (2003) 443.
[39] B.J. Finlayson-Pitts, J.N. Pitts, Chemistry of the Upper and Lower Atmosphere, Theory, Experiments and Applications, Academic Press, New York, 2000.
[40] M. Lieber, B. Smith, A. Szakal, W. Nelsonrees, G. Todaro, Int. J. Cancer 17 (1976) 62.
[41] H. Ishii, T. Fujii, J.C. Hogg, S. Hayashi, H. Mukae, R. Vincent, S.F. van Eeden, Am. J. Physiol. Lung Cell. Mol. Physiol. 287 (2004) L176.
[42] N.S. Holden, M.C. Catley, L.M. Cambridge, P.J. Barnes, R. Newton, Eur. J. Biochem. 271 (2004) 785.
[43] G.S. Hoare, A.H. Chester, M.H. Yacoub, N. Marczin, Int. J. Mol. Med. 9 (2002) 35.
[44] A.E. Haddrell, H. Ishii, S.F. van Eeden, G.R. Agnes, Anal. Chem. 77 (2005) 3623.
[45] A.E. Haddrell, S.E. van Eeden, G.R. Agnes, Toxicol. In Vitro 20 (2006) 1030.
[46] R.E. March, Rapid Commun. Mass Spectrom. 12 (1998) 1543.
[47] R. Vehring, C.L. Aardahl, E.J. Davis, G. Schweiger, D.S. Covert, Rev. Sci. Instrum. 68 (1997) 70.
[48] E.J. Davis, M.F. Buehler, T.L. Ward, Rev. Sci. Instrum. 61 (1990) 1281.
[49] E.J. Davis, Aerosol Sci. Technol. 26 (1997) 212.
[50] A.B. Turnbull, R.M. Harrison, Atmos. Environ. 34 (2000) 3129.
[51] C. Monn, S. Becker, Toxicol. Appl. Pharmacol. 155 (1999) 245.
[52] A. Nel, T. Xia, N. Li, Science 311 (2006) 622.